

Energy-Efficient and Context-Aware Smartphone Sensor Employment

Özgür Yürür, *Member, IEEE*, Chi Harold Liu, *Member, IEEE*, Charith Perera, Min Chen, *Senior Member, IEEE*,
Xue Liu, *Member, IEEE*, and Wilfrido Moreno

Abstract—New-generation mobile devices will inevitably be employed within the realm of ubiquitous sensing. In particular, smartphones have been increasingly used for human activity recognition (HAR)-based studies. It is believed that recognizing human-centric activity patterns could accurately enough give a better understanding of human behaviors. Further, such an ability could have a chance to assist individuals to enhance the quality of their lives. However, the integration and realization of HAR-based mobile services stand as a significant challenge on resource-constrained mobile-embedded platforms. In this manner, this paper proposes a novel discrete-time inhomogeneous hidden semi-Markov model (DT-IHS-MM)-based generic framework to address a better realization of HAR-based mobile context awareness. In addition, we utilize power-efficient sensor management strategies by providing three intuitive methods and constrained Markov decision process (CMDP), as well as partially observable Markov decision process (POMDP)-based optimal methods. Moreover, a feedback control mechanism is integrated to balance the tradeoff between accuracy in context inference and power consumption. In conclusion, the proposed sensor management methods achieve a 40% overall enhancement in the power consumption caused by the physical sensor with respect to the overall 85–90% accuracy ratio due to the provided adaptive context inference framework.

Index Terms—Context-aware framework, human activity recognition (HAR), optimal sensing, power efficiency.

I. INTRODUCTION

THE ever-increasing technical advances in embedded systems, together with the proliferation of growing development and deployment in small-size sensor technologies, have enabled smartphones to be repurposed to recognize daily oc-

curing human-based actions, activities, and interactions, which mobile device users encounter with the surrounding environment. Accurately recognizing human-related event patterns, which are called *user states*, can give a better understanding of human behaviors. Such recognition can also be used to assist individuals to enhance the quality of their lives. Therefore, the inference of a variety of human activities in a computationally pervasive way within a very diverse context has drawn much interest in the research area of ubiquitous sensing.

In the real world, being aware of context and communicating is a key part of human interaction. A context can be defined as characterization of a specific entity situation such as user profile, user surrounding, user social interaction, or user activity [1]–[3]. Applying context awareness into mobile devices enables to have a collection of autonomous, ambient intelligent, and self-operated network nodes (e.g., independently acting smartphones), which are well aware of surrounding context, circumstances, and environments. The evolution of ubiquitous sensing on resource-constrained mobile devices have empowered the creation of context-aware middleware [4], [5]. It emerges as a promising solution for the dynamic integration of highly complex and rich interactions among the virtual world and the physical world. With these capabilities, the new emerging network architecture would enhance data credibility, quality, privacy, and sharing ability by encouraging participation at personal, social, and urban scales, and would lead to the discovery of the knowledge about human lives and behaviors, and environment interactions/social connections by leveraging the deployment capacity of smart things (e.g., smartphones and tablets) to collect and analyze the digital traces left by users.

However, the heavy use of the built-in smartphone sensors would bring new challenges particularly in resource-constrained hardware platforms. Continuously capturing user context through sensory data acquisitions and inferring desirable hidden information from the context would put a heavy workload on the smartphone processor and sensors. Thereby, these operations cause more power consumption than the device itself does during a regular run. Eventually, smartphone battery would deplete rapidly.

To address power efficiency in context awareness, the best energy saving algorithm would be the one that infuses into the low-level sensory operations by manipulating the frequentness of sensory sampling intervals. In particular, an adaptive sensor management mechanism that dynamically assigns duty cycles (DCs) and sampling periods in a context-aware manner would reduce power consumption significantly. However, intervening sensory operations to achieve power efficiency jeopardizes the

Manuscript received February 17, 2014; revised June 17, 2014 and August 12, 2014; accepted October 17, 2014. Date of publication October 23, 2014; date of current version September 15, 2015. This work was supported in part by the National Natural Science Foundation of China under Grant 61300179. The review of this paper was coordinated by Dr. I. Krikidis. (Corresponding author: Chi Harold Liu.)

Ö. Yürür is with RF Micro Devices, Greensboro, NC 27409 USA (e-mail: oyurur@mail.usf.edu).

C. H. Liu is with Beijing Institute of Technology, Beijing 100081, China (e-mail: chiliu@bit.edu.cn).

C. Perera is with the Commonwealth Scientific and Industrial Research Organisation, Australian National University, Canberra, ACT 0200, Australia (e-mail: charith.perera@csiro.au).

M. Chen is with Huazhong University of Science and Technology, Wuhan 430074, China (e-mail: minchen@ieee.org).

X. Liu is with McGill University, Montreal, QC H3A 1Y1, Canada (e-mail: xueliu@cs.mcgill.ca).

W. Moreno is with the Department of Electrical Engineering, University of South Florida, Tampa, FL 33620-5399 USA (e-mail: oyurur@mail.usf.edu; wmoreno@usf.edu).

Color versions of one or more of the figures in this paper are available online at <http://ieeexplore.ieee.org>.

Digital Object Identifier 10.1109/TVT.2014.2364619

accuracy, i.e., quality of service, provided by context-aware services. Therefore, it creates a tradeoff between power consumption and accuracy provided by these services.

In this paper, we propose a novel framework that allows to run a HAR-based smartphone application while achieving a fine balance in the defined tradeoff. The framework consists of a context inference module, including an observation analysis block to acquire and infer the desired contexts through the smartphone accelerometer, a statistical machine to represent user activities, and a sensor management system to prolong the smartphone battery lifetime. Our objective is to improve the power efficiency of smartphones by dynamically adapting sensor sampling rates and DCs while supporting accurate recognition in user activities. More importantly, this research creates an effective hidden Markov model (HMM)-based framework that provides optimal power saving methods at the low-level sensory operations to guide the development of future context-aware applications. The following are a few distinctive key novelties exposed by this paper.

- User profiles are considered time-variant (inhomogeneity) in a provided statistical machine. Therefore, the adaptability problem is defined for time-varying user profiles, and a relevant solution is given by introduction of the entropy production rate. The entropy production rate is also used for the accuracy notifier in a context inference problem.
- The analytical modeling of the accelerometer sensor is provided and integrated into the sensor management system. The system aims at utilizing a mixture pair of duty cycling and adaptive sampling regulated by three intuitive and two suboptimal sampling policies to prolong mobile device battery lifetime.
- Missing observations occurred due to the power saving strategies that are estimated under the regulation of inhomogeneous semi-Markovian process.
- A feedback control mechanism is integrated between context inference module and sensor management system to ensure that a fine balance is obtained for the tradeoff.
- A smartphone application is implemented to show the effectiveness of proposed entropy production rate analysis on accuracy notification and the extension of battery lifetime under proposed sensor management system.

The remainder of this paper is organized as follows. Section II gives a relevant prior research. Section III provides the purpose and intention of the proposed framework design. Section IV explains the context inference module consisting of analysis of sensory data and the creation of a statistical machine to represent true user activities and behaviors. Section V includes the analytical model of sensor utilization, and power saving solutions to balance the tradeoff. Section VI is reserved for performance analysis. Finally, Section VII shows the conclusion and future work. In addition, the summary of important notations used throughout the paper is listed in Table I.

II. RELATED WORK

Pervasive mobile computing, which captures and evaluates sensory contextual information to infer user relevant actions/activities/behaviors, has been becoming a well-established re-

TABLE I
SUMMARY OF IMPORTANT SYMBOLS

Symbol	Definition (Section where the symbol is first used)
S_t	user state (IV-A)
S_s^τ	Markov chain, or sequence of user states (IV-A)
ϑ_t	observation (IV-A)
ϑ_s^τ	sequence of observations (IV-A)
o	observation emission matrix (IV-A)
n, s, t, τ	time indexes throughout the paper (IV-A)
i, j, m	indexes for user states (IV-A1)
ξ	inhomogeneous Markov process (IV-A1)
q_{ij}	user state transition rate (IV-A1)
Q	user state transition density matrix (IV-A1)
p_{ij}	user state transition probability (IV-A1)
P	user state transition matrix (IV-A1)
π_i	initial user state probability (IV-A1)
F_{ij}	probability of waiting time in a state (IV-A2)
H_i	probability of leaving a user state (IV-A2)
d_i	a random time distribution (IV-A2)
\mathcal{F}_j	filtered probabilities (IV-A3)
\mathcal{P}_j	predicted probabilities (IV-A3)
\hat{S}_t	estimation of user state (IV-A3)
N	total no. of user state transitions (IV-A4)
N_i	total no. of passages in a fixed user state (IV-A4)
e_p	instantaneous entropy production rate (IV-B)
ϕ	accuracy notifier (IV-B)
a	actions (IV-B)
t_{suff}	sufficient time to trigger an action (IV-B)
S^R , or S^{R^2}	1D, or 2D state space for reward process (V-A)
r, w	indexes for states $\in S^R$ (V-A)
l, k	indexes for $l \in DC$ and $k \in f_s$ (V-A)
$\Theta_{t_{span}}$	total power consumption for a spanning time (V-A)
ψ_{S^R}	reward process attached to ongoing S^R (V-A)
V	total received reward, i.e. power consumption (V-A)
u	optimal policies in CMDP and POMDP (V-D)
P^a	state transition matrix under actions (V-D)
I	identity matrix (V-D)
λ	belief vector (V-E)
R^a	rewards according to actions (V-E)

search domain, particularly within the realm of human activity recognition (HAR) and location-based services. Most studies rely on recognition of user activities (particularly posture detection) and definition of common user behaviors by proposing and implementing numerous context inferring systems. In addition, researchers have been aware of the need for computational power while trying to infer sensory context accurately enough. However, most works provide some partial answers to the tradeoff between context accuracy and battery power consumption. It is hard to say that power saving considerations have been significantly taken at the low-level physical sensory operations. In particular, there is no generic framework that intends to apply *adaptively changing* dynamic sensor management strategies, which employs varying DCs and sampling periods during a sensory operation similar to what this paper intends to propose.

From the standpoint of a creation of framework design in context-aware applications, it would be notable to mention the following studies. “EEMSS” in [6], “Jigsaw” in [7], “Sensay” in [8] and “SeeMon” in [9] use hierarchical sensor management strategy by powering a minimum number of sensors and applying fixed sensor DCs so that the proposed framework could recognize user states through smartphone sensors while improving device battery lifetime. Unfortunately, sensors have fixed DCs, and they are not adjustable to respond differently to variant user behaviors. In addition, energy consumption is reduced by shutting down unnecessary sensors at any particular

time. On the other hand, classification of sensory data is based on predefined test classification algorithms. Apart from these studies, many other works have emphasized to use deterministic sampling period schemes [10] and to maximize power efficiency by solely applying less complexity in computations or by changing transferring methods of inferred contextual data packets [9]. The other popular method is to fuse multiple sensory information to decide future employment of a specific sensor, particularly in localization applications [11], [12].

This paper differs from other studies in the following ways. First, this paper considers the physical world as inhomogeneous. Therefore, the inhomogeneity is characterized by time-variant system parameters. Second, the adaptability challenge in response to variant and rapid user activities is integrated as well using the convergence of entropy rate in conjunction with the inhomogeneity. Accordingly, the entropy rate is used to make an assumption on accurate working of system parameters regulated by an ongoing stochastic process. Third, power saving considerations are taken at the low-level sensory operations. Fourth, and most importantly, a machine learning structure regulates sensor management by estimating the trend of user preference, and opportunistically finding out stable moments in user activity. Thereby, sensor management could apply optimal sensing policies and change sensor sampling settings to respond the defined tradeoffs in context-aware application services. Finally, missing contextual inferences are estimated while energy saving strategies are being applied.

III. PROPOSED FRAMEWORK

Context-aware sensing systems have been put forward to provide a required model for recognition of daily occurring human activities via observations acquired by various sensors built in mobile devices. These activities are inferred as outcomes of a wide range of sensor applications utilized in such areas of environmental surveillance, assisting technologies for medical diagnosis/treatments, and creation of smart spaces for individual behavior model. Key challenges that are faced in this concept is to infer relevant activity in such a system that takes raw sensor readings initially and processes them until obtaining a semantic outcome under some constrictions. These constrictions mostly stem from difficulty of shaping exact topological structure and from modeling uncertainties in the observed data due to saving energy wasted while physical sensor operations and processing of data are being undergone. Finally, there is no common framework system that covers all types of application settings, provides an adaptation toward changing context, and acquires a collection of asynchronous heterogeneous context to create different abstract entities. None of current frameworks succeeds to have a full transparency, which eliminates a direct involvement of applications into context modeling process, by imposing less computational workload on resource-limited mobile devices. In this direction, gathering diverse and asynchronous information and presenting it to the application would be the future work in context-aware framework research, which this paper intends to enlighten. By this means, this paper could help the exciting vision of "Internet-of-Things" [13] while creating a knowledge

network capable of making autonomous logical decision to actuate environmental objects, as well as to assist individuals, particularly in a resource-constrained smart device. In addition, this paper could give a solution to effectively manage fusion of data gathered from multiple sensor applications.

To this end, this paper proposes an inhomogeneous (time-variant) HMM-based framework to represent HAR-based user states by defining them as an outcome of either recognition or estimation model. A statistical tool-based classification, mostly using HMMs [14], [15] or using autoregressive (AR) [16] models, is one of the foremost methods to infer context obtained via wearable or built-in smart device sensors in HAR-based applications. However, these studies mostly allow predefined and *user-manipulated* system parameter settings, such as arbitrary formation of context transition matrix in HMMs or building filtering coefficients in AR models, which is not suitable for online processing due to increasing computational workload while enlarging the data size. Therefore, a statistical model is added into our approach to track *time-variant* user activity profiles to predict the best likely user state that fits into instant user behavior. The inhomogeneity is characterized by time-variant system parameters, and the user profile adaptability challenge is modeled using the convergence of entropy rate. Accordingly, an implemented smartphone application is provided to demonstrate how entropy rate converges in response to distinctive time-variant user profiles under different sensory sampling operations. The proposed framework is designed to be based on a statistical machine to obtain a better realization in context awareness to create adaptability to time-variant user preferences and behaviors, estimate missing context inferences in presence of idle sensory operations, and preserve the functionality against aperiodically received sensory observations.

Most importantly, the key of this study is that a machine learning structure regulates sensor management opportunistically to figure optimal sensing policies and changes sensor sampling settings, such as varying sensory sampling and duty cycling, to achieve power efficiency while satisfying the accuracy of context-aware application services.

The following two sections give further information about two interoperated core modules that our proposed framework has: context-inference module and sensor management system.

IV. CONTEXT INFERENCE MODULE

The proposed context inference module consists of two main blocks as shown in Fig. 1, which are sensory data acquisition and analysis, and a statistical machine. The first block receives *raw sensory readings* (i.e., extracted user contexts through mobile-device-based sensors) as *inputs*. These readings undergo a series of signal processing operations, and eventually end up with a classification algorithm to provide desirable inferences about user-relevant information for context-aware applications. Note that the selection of classification algorithm in the inference process could differ due to the interested context obtained through a target sensor. The probabilistic outcomes of the classification algorithms source the inputs of the second block.

The second block chooses a discrete-time inhomogeneous hidden semi-Markov model (DT-IHS-MM) as the desired

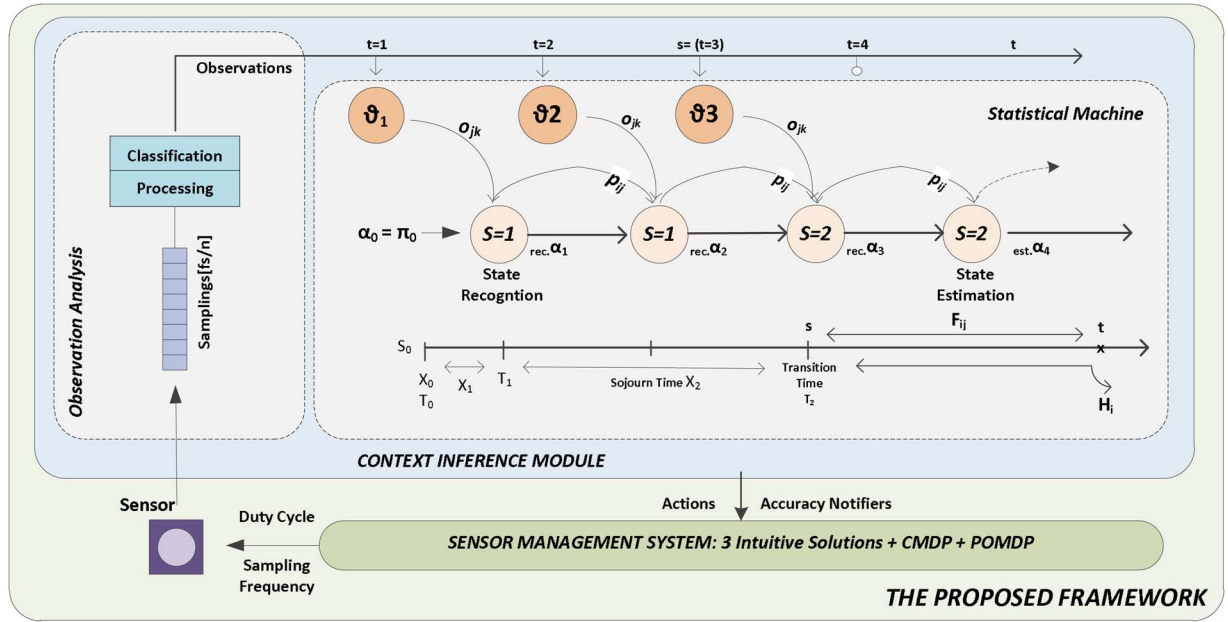


Fig. 1. Operational process flow of the proposed context-aware framework: The framework consists of two main modules, which are context inference module and sensor management system. Basically, context inference module acquires sensory data, extracts context, infers user states, and delivers recognition accuracy statistics to sensor management system. Then, sensory operations are adjusted by sensor management system to achieve a fine balance in power consumption and recognition accuracy.

statistical machine. HMMs have been used to infer mobile-device-based human-centric sensory context in HAR-based applications [17]. However, our approach intends to expand the properties of statistical machine so as to obtain a better realization in context awareness. First, the concept of Markov renewal process is adopted to describe the functionalities of user behavior modeling. Second, the inhomogeneity is introduced to characterize time-variant user behaviors so that the module could adapt itself to dynamically changing user behaviors. Third, the semi-Markovian feature is added to specify aperiodically received discrete-time observations through sensory readings. Fourth, the estimation theory is included in case of missing sensory inputs. Finally, the entropy rate analysis is integrated to track the accuracy of context inferences because there is not an absolute solution to actually calculate the accuracy of a real-time running HAR-based context-aware application. Thereby, *the convergence of entropy rate* is considered *output* of the module, which will be used by the sensor management system introduced in Section V.

The following subsections include the explanations of main blocks in context inference module. The desirable statistical machine is put forward first since some system parameters declared in this block will be used during the introduction of the subsequent sensory data acquisition and analysis block.

A. Inhomogeneous Hidden Semi-Markov Model: A Statistical Machine

Classification algorithms produce observations (i.e., *visible states*) ϑ_t of DT-IHS-MM. Among given observations, the one that has the highest probability will make a most likely differentiation in the selection of instant user behavior. This observation is marked as instant observation ϑ_T , which also indicates the

most recent element of observation sequence ϑ_1^T of DT-IHS-MM. On the other hand, user states, *sitting*, *standing*, *walking*, and *running*, are defined as *hidden states* S of DT-IHS-MM since they are not directly observable but only reachable over visible states. Therefore, each observation has cross probabilities to point a user state. These cross probabilities build an observation emission matrix o , which basically defines decision probabilities to pick any user states from available observations.

In addition, the transition probabilities among user states might not be stationary since a general user behavior changes in time. Thus, it is expected from a user state either to transit into another user state or to remain in the same with a different probability. These occurrences build a time-variant user-state transition matrix p .

1) *Basic Definitions and Inhomogeneity:* Let an inhomogeneous Markov process exist as $\xi = \{\xi(t), t \geq 0\}$ with a user-state space of $S = \{1, 2, \dots, M\}$, and let $Q(t) = q_{ij}(t)$, where $\{i, j\} \in S$, and $t \geq 0$ be a transition density matrix of ξ . If Q satisfies both $0 \leq q_{ij}(t) \leq \infty$ and $q_i(t) = -q_{ii}(t) = \sum_{i \neq j} q_{ij}(t)$, then Q is called a conservative inhomogeneous transition density matrix function on S .

$q_{ij}(t)$ represents jump or transition rates from user state i to user state j at time t . Whenever $i = j$, it means that current user state remains unchanged or a dummy transition occurs.

Moreover, suppose that a user-state transition probability matrix $P(s, t) = \{p_{ij}(s, t) = \Pr(S(t) = j | S(s) = i)\}$, where $t \geq s \geq 0$, together with Q , satisfies both forward and backward Kolmogorov's equations [18], which assume to have $\lim_{t \downarrow s} \partial p_{ij}(s, t) / \partial t = q_{ij}(s)$, then S becomes an *inhomogeneous Markov chain* with the transition density of Q . The chain can revisit a user state at different system times, and not every user state needs to be visited. Hence, there is no requirement that user-state transition probabilities must be symmetric

($p_{ij} \neq p_{ji}$) or a specific state might remain the same in succession of time ($p_{ii} = 0$).

Furthermore, let an initial user state $\pi(t) = \{\pi_i(t) = \Pr(S(t) = i)\}$ satisfy the Fokker-Planck equation [18] $d\pi(t)/dt = \pi(t)Q(t)$.

2) *Working Process*: Let $\xi = \{\xi_n, n \in \mathbb{N}\}$ be redefined as an inhomogeneous irreducible discrete Markov process with a user-state space of S . The process evolves from S_0 as an initial user state and stays in there for a nonnegative length of time X_1 until it goes into another user state S_1 . Then, it stays in the new user state for X_2 before entering into S_2 and so on. As indicated in [19], this process is a 2-D or bivariate stochastic process in discrete time called positive ($S - X$) process: $(S - X) = ((S_n, X_n), n \geq 0)$ with initial of $X_0 = 0$, where X_n is called the successive sojourn times.

X_n is the time spent in state S_{n-1} that defines interarrival times. There is also another time variable T_n introduced for the definition of system properties at which state transitions occur. This random time sequence is called renewal sequence, and it is given by $X_n = T_n - T_{n-1}, n \geq 1$ with the initial statuses of $\{X_0, T_0\} = \{0, 0\}$.

The Markov renewal process is now redefined over $(S - T) = ((S_n, T_n), n \geq 0)$ by

$$Q_{ij}(s, t) = \Pr(S_{n+1} = j, T_{n+1} \leq t | S_n = i, T_n = s) \quad (1)$$

where T_n represents the n th renewal time at which a user-state transition occurs.

The probability of waiting time, also called conditional distributions of sojourn times, for each user state i in the presence of (1) and information about the successively followed user state is given by

$$F_{ij}(s, t) = \Pr(T_n \leq t | S_{n-1} = i, S_n = j, T_{n-1} = s) \\ = \begin{cases} Q_{ij}(s, t)/p_{ij}(s), & p_{ij} \geq 0 \\ 1, & p_{ij} = 0. \end{cases} \quad (2)$$

In addition, with the help of (1) and (2), the probability of the process leaving the user state i , which is also called sojourn time distributions in a given user state, from time s to t is introduced by

$$H_i(s, t) = \Pr(T_n \leq t | S_{n-1} = i, T_{n-1} = s) \\ = \sum_j p_{ij}(s) F_{ij}(s, t) = \sum_{j \neq i}^U Q_{ij}(s, t). \quad (3)$$

If $F(s, t) = F(t - s), s \leq t$, then the kernel Q only depends on $t - s$, which it yields to have $Q(t - s) = pF(t - s)$ being called an inhomogeneous semi-Markov process. The semi-Markov process [20], [21] indicates that the sojourn time belonging to each state might have a random distribution $d_i(t)$ ¹, which can depend on the next user state to be visited. Thereby, this gives the probability of a user-state transition being occurred at time t , i.e.,

$$b_{ij}(s, t) = \begin{cases} Q_{ij}(s, t) = 0, & t \leq s \\ Q_{ij}(s, t) - Q_{ij}(s, t - 1), & t > s. \end{cases} \quad (4)$$

¹The proposed solutions in Section V regulate sampling epoch times in sensory operations and change the defined time distribution accordingly.

Moreover, for each waiting time, a user state is occupied. Therefore, transition probabilities are defined with (3) and (4) by

$$p_{ij}(s, t) = \Pr(S_t = j | S_s = i) = \delta_{ij} (1 - H_i(s, t)) \\ + \sum_{m \in M} \sum_{\tau=1}^t b_{im}(s, \tau) p_{mj}(\tau, t) \quad (5)$$

where δ_{ij} represents the Kronecker symbol. The first element on the right-hand side, where $d_i(t) = 1$ if $i = j$, notifies the probability of residing in user state i at time t without any change in context since time s , and the second element represents the probability of a user-state transition from state i in some way to user state j , and staying in this new user state at time t , i.e.,

$$\alpha_j(s, t) = \sum_{t'=s}^t \sum_i \left[\alpha_i(s, t - t') p_{ij}(s, t - t') d_j(t') \right. \\ \left. \prod_{t''=1}^{t'} o_j(\vartheta_{t-t'+t''} = z) \right]. \quad (6)$$

3) *User-State Representation Engine*: User-state representation engine infers an instant user behavior in light of prior knowledge of a human behavior pattern and the availability of sensory observation at a decision time. If sensory observation exists, the applied process is called recognition method; otherwise, an estimation method is used. In other words, the estimation method is applied due to missing observations when power efficiency is taken into consideration at the low-level sensory operations.

Let ϑ_t denote an observation at time t , which is associated with user state S_t , and let $o_i(\vartheta_t)$ be the probability of observing ϑ_t from given $S_t = i$. Thus, $o_i(\vartheta_s^T) = \prod_{t'=s}^T o_i(\vartheta_{t'})$ represents a sequence of emitted observations from time s to $t, s \leq t$. In addition, note that since the process flows in a discrete time and follows the first-order Markovian feature, a current user state S_t depends solely on the most recent user state S_{t-1} .

The inference of a hidden user state j at time t , given the last known hidden user state i at time $s, s \leq t$, is presented by

$$\Pr(S_t = j | S_s = i, \vartheta_s^\tau) \quad (7)$$

where $\tau = t - s$. Equation (7) is termed as *predicted \mathcal{P} , filtered \mathcal{F} , and smoothed \mathcal{S}* probabilities of S_t , depending on observation sequence of $\vartheta_s^{t-1}, \vartheta_s^T$, or ϑ_s^T , respectively where $T > t$.

The recognition method uses filtered probabilities of S_t where it is derived from (7) as in $\mathcal{F}_j(s, t) = \Pr(S_t = j | S_s = i, \vartheta_s^T)$ in the presence of sufficient number of available observations. The probability of an instant user-state recognition is found by the forward algorithm [17], which is proposed to find the most likely one-step-ahead user state in a hidden chain. The forward algorithm relies on updating a probability weight α inductively, which decides the probability of current occurrence of a user state S_t generated from the one-step-previous occurrence S_{t-1} . However, this method works well for traditional HMMs and not for Semi-Markovian featured models due to the random sojourn time distribution between two consecutive

user states in the hidden chain. In this manner, an extended forward algorithm has been proposed in [22] and [23] by (6) with the condition of $\alpha_i(s, t) = \pi_i$ if $t \leq 0$.

Since the recognition process of user states evolves in real time, the forward algorithm assigns a proper user state to specify current user activity in case where a new observation is made. On the other hand, to make sure that user-state recognitions are made true, the backward algorithm, whose corresponding weight is denoted by β , is employed [17]. By this algorithm, the accuracy of previous user-state recognitions is validated, i.e., *smoothing*. However, applying this algorithm seems redundant as it consumes additional computational power on the mobile device batteries. The context-aware applications run in real time, thereby there is no value of discovering what happened in the past again. Hence, the backward component can be neglected, and the filtered probability becomes

$$\mathcal{F}_j(s, t) = \alpha_j(s, t)\beta_j(s, t') = \alpha_j(s, t), \quad t = t' = T. \quad (8)$$

Note that computational complexity while calculating system parameters causes a crucial underflow problem. When time goes by during evolution of ξ , $\alpha_i(0, t) \xrightarrow{t} 0$ starts to head to zero at an exponential rate since p_{ij} includes elements being lower than 1. Therefore, $\mathcal{F}_j(s, t)$ needs to be scaled [17] by a factor of $\prod_{t'=s}^t \sum_j \mathcal{F}_j(s, t')$.

In addition to using the filtered probabilities to recognize user states, the predicted probabilities are used to estimate user state in case of no observation received. When power saving methods are taken into consideration as studied in Section IV-B, there will be some time intervals during sensory operations in which no sensor readings are obtained. As a result, the framework cannot receive a relevant observation. In that case, the inference of instant user state is based on the estimation method and not on the recognition method.

The predicted probabilities are found by

$$\begin{aligned} \mathcal{P}_j(s, t) &= \Pr(S_t = j | S_s = i, \vartheta_1^{t-1}, \vartheta_t) \\ &= \Pr(S_t = j, \vartheta_t = z | S_s = i, \vartheta_1^{t-1}) \\ &= \sum_j \mathcal{F}_i(s, t-1) p_{ij}(s, t-1). \end{aligned} \quad (9)$$

Alternatively, (9) can be found by assigning the most likely visionary observation instead of accepting that there is a missing observation, i.e.,

$$\mathcal{P}_{j,z}(s, t) = \sum_j \mathcal{F}_i(s, t-1) p_{ij}(s, t-1) o_j(\vartheta_t = z). \quad (10)$$

Then, the most likely observation is selected according to assigning each possible observation as a final node to observation sequence while calculating (10) by

$$\hat{\vartheta}_t = \arg \max_z \sum_j \mathcal{P}_{j,z}(s, t). \quad (11)$$

Finally, the instant user-state estimation is found using (10) together with (11) by

$$\hat{S}_t = \arg \max_{1 \leq j \leq M} [\mathcal{P}_{j,z}(s, t)]. \quad (12)$$

Then, instant user-state recognition is specified using (8) in case where observations are available by

$$S_t = \arg \max_{1 \leq j \leq M} [\mathcal{F}_j(s, t)]. \quad (13)$$

4) *Time-Variant User-State Transition Matrix*: The most important feature of context-aware applications is being capable of adapting themselves to distinctive user behaviors. User-relevant context differs in time and the corresponding user state also does. For instance, one user might remain the same user state for a long time, whereas others might be more active by changing their user states frequently. Therefore, it cannot be expected from user-state transition matrix to remain stationary under such conditions.

- *Default Settings*: User-state transitions can be represented as simple random walk on a graph [24]. On this graph, vertex v represents a user state, and an edge represents a user-state transition. Thus, ξ always starts evolving by a default transition matrix, which is

$$p_{ij}^{\text{default}} = \frac{1}{d(v_i)}, \quad v_i \sim v_j \quad (14)$$

where $d(v_i)$ is the number of vertices v_j adjacent to v_i . For example, if $d(v_i)$ is 0, $p_{ii}^{\text{default}} = 1$, i.e.,

$$\begin{aligned} p_{ij}(s, \tau_0, \tau) &\stackrel{\text{update}}{=} \delta_{ij} (1 - H_i^*(s, \tau_0, \tau)) \\ &+ \sum_{m \in M} \sum_{v=\tau_0}^{\tau} b_{im}^*(s, \tau_0, v) p_{mj}(s+v, \tau-v). \end{aligned} \quad (15)$$

- *Update*: A random variable $N(t) > n - 1 \leftrightarrow T_n \leq t$ is represented as the total number of jumps or transitions of the $(S - T)$ process during $(s = 0, t]$. Therefore, $N(t)$ is also called the discrete-time counting process of the number of jumps. Jumps or transitions may include any transition towards user state itself (i.e., virtual transitions).

By having the counting process, counting parameters can be calculated, where $0 < \tau \leq t$, as follows.

- The number of visits to user state i during $(0, t]$: $N_i(t) = \sum_{n=0}^{N(t)-1} \mathbf{1}_{\{S_n=i\}}$.
- The number of transitions from user state i to user state j during $(0, t]$: $N_{ij}(t) = \sum_{n=1}^{N(t)} \mathbf{1}_{\{S_{n-1}=i, S_n=j\}}$.
- The number of transitions from user state i to user state j during $(0, t]$ with the sojourn time τ in state i : $N_{ij}(\tau, t) = \sum_{n=1}^{N(t)} \mathbf{1}_{\{S_{n-1}=i, S_n=j, X_n=\tau\}}$.

The empirical estimations of the user-state transition matrix p_{ij} , the conditional distributions of sojourn times f_{ij} , and the discrete-time semi-Markov kernel q_{ij} are given in [25] by

$$\begin{aligned} \hat{p}_{ij}(t) &= N_{ij}(t)/N_i(t), \quad \hat{f}_{ij}(\tau, t) = N_{ij}(\tau, t)/N_{ij}(t) \\ \hat{q}_{ij}(\tau, t) &= N_{ij}(\tau, t)/N_i(t). \end{aligned} \quad (16)$$

The given empirical estimations in (16) approach nonparametric maximum likelihood estimations with having good

asymptotic properties if they maximize the likelihood function of

$$\mathcal{L}(t) = \prod_{n=1}^{N(t)} p_{ij} f_{ij}(X_n) \left(1 - \sum_j \sum_{\tau=n}^{B(t)} q_{ij}(\tau) \right) \quad (17)$$

where $B(t) = t - X_{N(t)}$ is called the age process showing the sojourn time in the last visited state $S_{N(t)}$.

With the evaluation of (17), the corresponding transition density kernel turns into

$$Q_{ij}(s, \tau_0, \tau) \stackrel{\text{update}}{=} \frac{Q_{ij}(s, \tau) - Q_{ij}(s, \tau_0)}{Q_{ij}(s, \tau_0)} \quad (18)$$

where τ_0 is the elapsed time since the first entrance into user state i .

Finally, beginning from the default status in (14), the evolving inhomogeneous state transition probability (5) is updated by (18) together with (3) and (4) as in (15).

5) *Observation Emission Matrix*: The least power-consuming sensor on today's smartphones is the accelerometer [11]. Therefore, the accelerometer sensor is considered used in the implementation of HAR-based applications. Blackberry RIM Storm II 9550 smartphone is chosen target device. Storm II consists of three-axis accelerometer named ADXL346 from Analog Devices [26]. While any application is running, the target smartphone is only connected to a Third-Generation (3G) network, and background operations are kept at minimum.

For performance evaluations, first, two user states, which are *sitting* and *standing*, and four user states, which are *sitting*, *standing*, *walking*, and *running*, consisting statistical machines are considered for the framework. However, more complex models can be applied as well by using similar system approach. In our previous work [27], an unsupervised classification method to detect user-centric postural actions, such as sitting, standing, walking, and running, by smartphones is studied. By adopting these works into our current study, recognition between user states is made. Then, the observation emission matrix for two and four user states are constructed by adopted algorithm as

$$o_{jz} = \begin{bmatrix} \text{prob. of sitting} \\ \text{prob. of standing} \end{bmatrix}, \begin{bmatrix} \text{prob. of sitting} \\ \text{prob. of standing} \\ \text{prob. of walking} \\ \text{prob. of running} \end{bmatrix}. \quad (19)$$

B. Output of the Context Inference Framework

Supposing $\pi_i(0) > 0$ where $\forall i \in S$, the Markov process ξ_n evolves in bidirectional way over the distributions of $P_{[n, n+\hat{n}]}$ and $P_{[n, n+\hat{n}]}$, where $\forall n \in \mathbb{Z}^+$ and $\forall \hat{n} \in \mathbb{N}$, and the user-state transition matrix also obeys a condition of $p_{ij} > 0 \leftrightarrow p_{ji} > 0$, then ξ_n satisfies

$$\lim_{t \downarrow s} \frac{\pi_i(s) p_{ij}(s, t)}{\pi_j(s) p_{ji}(s, t)} = 1 \quad (20)$$

which indicates that the inhomogeneous Markov process has instantaneous reversibility at time s ; hence, it yields $\pi(s)Q(s) = 0$.

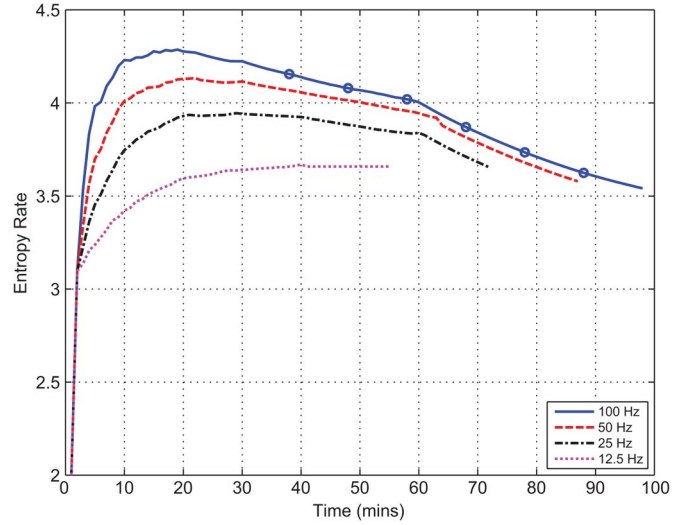


Fig. 2. Entropy rate analysis. The convergence of entropy production rate might differ depending on how accurate the context inference is made under different sampling frequencies.

Having the reversibility feature defined by (20), the instantaneous entropy production e_p^n of ξ at time n is given by

$$\begin{aligned} e_p^n &= \mathcal{H}(P_{[n, n+1]}, \bar{P}_{[n, n+1]}) \\ &= \frac{1}{2} \sum_{i, j \in S} [\pi_i^n p_{ij}^n - \pi_j^n p_{ji}^n] \log \frac{\pi_i^n p_{ij}^n}{\pi_j^n p_{ji}^n} \end{aligned} \quad (21)$$

where $\mathcal{H}(P_{[n, n+1]}, \bar{P}_{[n, n+1]})$ is the relative entropy of distribution of (ξ_n, ξ_{n+1}) , $P_{[n, n+1]}$, with respect to the distribution of (ξ_{n+1}, ξ_n) , $\bar{P}_{[n, n+1]}$.

By using (21), Fig. 2 shows the convergence of entropy rate under some sensory operation parameters, such as a fixed DC $DC = 1$ along with variant sampling frequencies $f_s = \{100, 50, 25, 12.5\}$ Hz. The aggressive sampling method, which takes 100 Hz as f_s , draws an actual track of the entropy rate. Circles over the blue line indicate a difference in user behavior. Since user states, such as sitting and standing, are recognized in this application example, the frequentness of transition from one user state to another cannot be observed much due to the nature of human being, which requires high energy effort by users throughout the application running time. Therefore, user-state transition matrices over time are desired as $p_{ij} = \begin{bmatrix} 0.9 & 0.1 \\ 0.1 & 0.9 \end{bmatrix}$, $\begin{bmatrix} 0.85 & 0.15 \\ 0.1 & 0.9 \end{bmatrix}$, $\begin{bmatrix} 0.8 & 0.2 \\ 0.1 & 0.9 \end{bmatrix}$, $\begin{bmatrix} 0.75 & 0.25 \\ 0.1 & 0.9 \end{bmatrix}$, $\begin{bmatrix} 0.6 & 0.4 \\ 0.1 & 0.9 \end{bmatrix}$, $\begin{bmatrix} 0.5 & 0.5 \\ 0.1 & 0.9 \end{bmatrix}$.

According to the results obtained by a HAR-based smartphone application, the entropy rate converges late while samplings are collected at less than 100 Hz. This indicates the reason why accuracy ratio decreases as well. In addition, the entropy rate cannot sometimes converge into any point and stops, where the plot lines belonging to $f_s = \{12.5, 25, 50\}$ Hz. When the frequentness of user-state transitions increases, sampling frequency may not be fast enough to capture the activeness of a user profile. Therefore, the system cannot find any proper user-state transition matrix to define instant user activity profile.

After all these assessments on the characteristic of entropy rate analysis with respect to a changing user activity profile, let

$e_p(s, t)$ denote a sequence of entropy rates from (21) in the time range of s up to t . Moreover, assume that a simple threshold is defined by $\varepsilon_{e_p} = [\mu_{e_p} - \sigma_{e_p}, \mu_{e_p} + \sigma_{e_p}]$, where μ_{e_p} and σ_{e_p} are the mean and standard deviation of $e_p(s, t)$, respectively. Thereby, the first output delivered to the sensor management system by the statistical machine as shown in Fig. 1 is named as accuracy notifier, which is defined by

$$\phi(s, t) = \frac{1}{(t - s + 1)} \sum_{n=s}^t \mathbf{1}_{(e_p^n \in \varepsilon_{e_p})}. \quad (22)$$

Moreover, τ_{ii} denotes a return time, i.e., elapsed total sojourn time, to user state i entering at s , as

$$\tau_{ii} = \begin{cases} \min\{n = t - s, n \geq 1, S_t = i | S_s = i\} \\ \infty, S_t \neq i, t \geq 1 \end{cases} \quad (23)$$

represents the amount of time until the process returns to the same user state i given the fact that it started from user state i . Note that it may never return back to the same state i .

By considering that a time variable t_{suff} is assigned during application run to indicate a sufficient time interval in which user state i would not change, the second output is defined then using (22) and (23) by

$$a(t) = \begin{cases} 1, & \phi(s, t) \geq \phi, \tau_{ii} > t_{\text{suff}} \\ 2, & \phi(s, t) \geq \phi, \tau_{ii} \leq t_{\text{suff}} \\ 3, & \phi(s, t) < \phi \end{cases} \quad (24)$$

where $\phi \in [0.5, 1]$, and $a(t)$ denotes the actions for sensory management introduced in Section V-B.

V. SENSOR MANAGEMENT SYSTEM

Here, the effect of variant sensory load profiles on the depletion of mobile device battery is studied. Then, these battery discharge profiles are examined within the concept of the Markov reward process. In addition, there are five novel solutions provided here for balancing the tradeoff existing between accuracy in the user-state recognitions and power consumption required by the recognition process.

A. Sensor Utilization

The smartphone accelerometer sensor is utilized to examine the power efficiency achieved under different sampling and duty cycling strategies. Assume that a set of DC and a set of f_s are given by $\{1, 0.75, 0.5\}$ and $\{100, 50, 25, 12.5\}$ Hz, respectively. Moreover, let a state space lie over two subspaces, which are sets of DC and f_s , as in $S^{R^2} = \{\text{DC} \times f_s\}$. Thus, the state space is defined as in

$$S_r^R = S_{\{l,k\}}^{R^2} = \left\{ S_{\{1,100\} \rightarrow 1}^{R^2}, S_{\{1,50\} \rightarrow 2}^{R^2}, \dots, S_{\{0.5,12.5\} \rightarrow W}^{R^2} \right\} \quad (25)$$

where $S^{R^2} \rightarrow S^R : \{\text{DC} = l, f_s = k\} \rightarrow r, \forall l \in \text{DC}, \forall k \in f_s$ and $W = \text{length}(\text{DC}) \times \text{length}(f_s)$.

The state space S^R or S^{R^2} is considered to represent different sensory operation methods supported by the accelerometer sensor in a sensor management system.

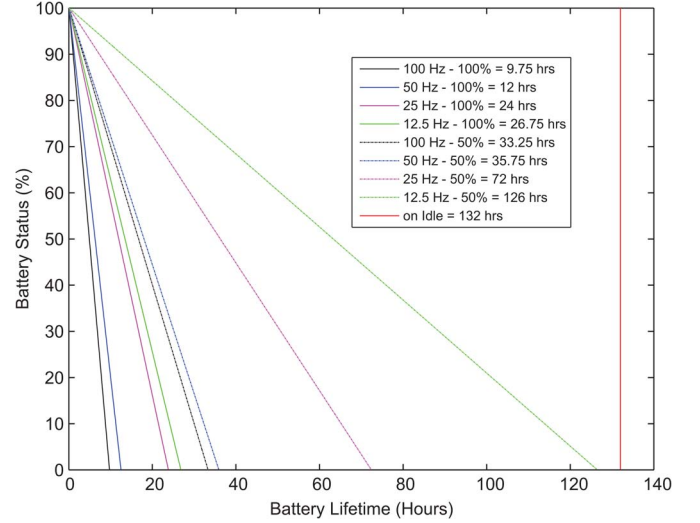


Fig. 3. Battery lifetime analysis. The total lifetime for battery depletion differs due to variant sensory operation methods within the smartphone accelerometer. Experiment values are taken at every 20-min time intervals.

To be able to see the effect of S^R on the battery depletion, an application is implemented on the target device. The application runs from a point where the smartphone battery is fully loaded until it totally depletes. Only one constant pair of sampling frequency and DC, i.e., a state in S^R , is applied as sensory operation parameters to the accelerometer at each application run. A total time for sensory operation cycle, which is denoted t_c , is taken as 1 s. For instance, where $f_s = 100$ Hz, DC = 100%, and $t_c = 1$ s are taken, the total number of samplings per second becomes 100.

The application results are shown in Fig. 3. Note that the Blackberry Java 7.1. SDK only reveals the remaining battery status. According to results, the more aggressive is sampling methodology applied, the faster the battery depletes. In addition, the lower value of DC makes the battery recover effect more significant, thus prolonging the battery lifetime. However, the battery nonlinearities [28] are not intended to be studied in this paper.

After the application results shown in Fig. 3 together with [26] and our previous work [29], the sampling-frequency-and-DC-dependent power consumption model in the accelerometer sensor operations can be defined as

$$\begin{aligned} \Theta_{\omega * 12.5 \text{ Hz}} &= \omega * \Omega_{\text{sample}} + (\omega_{\text{max}} - \omega) * \Omega_{\text{idle}} \\ \Theta_{t_c} &= \frac{(\text{DC})t_c}{\omega_{\text{max}}/f_{s_{\text{max}}}} \Theta_{\omega * 12.5 \text{ Hz}} + \frac{(1 - \text{DC})t_c}{1/f_{s_{\text{max}}}} \Omega_{\text{idle}} \end{aligned} \quad (26)$$

where $\omega = \{1, 2, 4, 8\}$; Ω_{sample} and Ω_{idle} are defined as the power consumption that occurred during the operations where sensor makes samplings or runs idle, respectively; and t_c is the time span through a power cycle.

By using (26) and the application results obtained for Fig. 3, Table II shows power consumption ratio of each sensory operation methods by the accelerometer, where the least aggressive sampling method, i.e., DC = 50% and $f_s = 12.5$ Hz, is taken as a normalizing factor.

TABLE II
POWER CONSUMPTION RATIO IN SENSOR DRAIN PER EACH
OPERATION CYCLE: $t_c = 2$ s, AND COMPARISONS
ARE APPLIED BASED ON (50%, 12.5 Hz)

(DC in %, f_s at Hz)	Ratio
(100, 100)	4.45
(50, 100)	2.58
(100, 50)	2.85
(50, 50)	1.80
(100, 25)	1.75
(50, 25)	1.24
(100, 12.5)	1.26
(50, 12.5)	1

To this end, assume that a semi-Markov chain represents the evolution of changing sensory operation methods S^R for a desired sensor management system. The chain consists of a finite state space $S^R = \{1, \dots, W\}$, the state transition density matrix $q^R \in Q^R$, and the state transition matrix $p^R \in P^R$, where $Q^R, P^R \in \mathbb{R}^{W \times W}$. In addition, a reward structure can be attached to this on-going chain, and it can be thought as a random variable associated with the state occupancies and transitions. Moreover, assume that the reward, denoted by ψ , is seen as power consumption per unit time while a mobile device battery is discharging, and S^R is redefined as the battery discharge profiles/states. Thereby, the total reward, i.e., total power consumption, depends on the total visiting time in a state r where $r \in S^R$. Then, it can be said that the reward ψ_r belonging to state r is proportional to the corresponding power consumption defined by (26).

Finally, the general evolution of a semi-Markov reward process to describe power consumption caused by sensory operations in the sensor management system is given by

$$V_w(s, t) = V_r(s, t - 1) + \sum_{w \in W} p_{rw}^R(s, t - 1) \psi_w(s, t) \quad (27)$$

where the left-hand side V represents the expected present value of all received rewards from time s to t given that the process enters into state i at time s , whereas the first element of the right-hand side represents the aggregation of rewards earned both at previous time, and the second element is the reward obtained from either continuity in the same state or transition to another state.

B. Tradeoff Analysis: The Description of Action Set

There are five different solutions proposed to respond to the defined tradeoff between sensing accuracy and power consumption. The proposed solutions aim at reducing power consumption by intervening sensory operations. Therefore, the context inference framework always receives the manipulated sensory samplings and then tries to recognize user states accurately according to (12) and (13). After the recognition process is done, it releases $a(t)$ as in (24), which defines actions to be taken on sensory operations. These actions force the proposed solutions to adjust a pair of DC or sampling frequency dynamically while sensory sampling operations are actively operated. As a result, a feedback system is integrated into a cyber-physical sensor management system that balances the increase in power efficiency with the decrease in user-state recognition accuracy.

Actions are defined as commands $\{1, 2, 3\}$ for sensor management, which are to *decrease*, *preserve*, and *increase* power consumption, respectively. If the entropy rate is not stable, which means user profile changes frequently, thereby corresponding entropy rate does not converge a specific value. Action #3 needs to be taken in this case to increase the power consumption in sensory operations by making more aggressive samplings. In contrast, if the entropy rate converges and hangs in a specific margin, then action #2 preserves the same setup for applied sensory operations. More significantly, if the same user profile has been observed at least for a sufficient time t_{suff} , then action #1 is taken to reduce power consumption by estimating that user profile is expected to stay on hold.

C. Intuitive Solutions

Intuitive solutions either reduce power consumption by decreasing DC or/and f_s , or improve accuracy in user-state recognition by increasing them. Relevant adjustments are regulated by action set of $a(t)$. There are three different intuitive solutions, as proposed in the following.

1) *Method I*: This method tries to change DC in the first place rather than to change f_s . Let the pairs of DC and f_s lie over a space S^{R^2} , which is defined in a matrix of $\{\text{DC}, f_s\} \rightarrow \{l, k\}$, where $l \in \text{DC}$ and $k \in f_s$. Method I (MI) proposes how to wander over the defined space according to actions by

$$S^{R^2}(l, k) = \begin{cases} S^{R^2}(l - 1, k), & a = 1, l \neq l_{\min} \\ S^{R^2}(l, k - 1), & a = 1, l = l_{\min}, k \neq k_{\min} \\ S^{R^2}(l + 1, k), & a = 3, l \neq l_{\max} \\ S^{R^2}(l, k + 1), & a = 3, l = l_{\max}, k \neq k_{\max} \\ S^{R^2}(l, k), & \text{otherwise.} \end{cases} \quad (28)$$

2) *Method II*: This method, in contrast to MI, makes the adjustments in f_s in the first place. Then, the relevant state transitions over S^{R^2} become

$$S^{R^2}(l, k) = \begin{cases} S^{R^2}(l, k - 1), & a = 1, k \neq k_{\min} \\ S^{R^2}(l - 1, k), & a = 1, k = k_{\min}, l \neq l_{\min} \\ S^{R^2}(l, k + 1), & a = 3, k \neq k_{\max} \\ S^{R^2}(l + 1, k), & a = 3, k = k_{\max}, l \neq l_{\max} \\ S^{R^2}(l, k), & \text{otherwise.} \end{cases} \quad (29)$$

3) *Method III*: In this method, state transitions are executed according to the ascending order of power consumption ratios shown in Table II. The definition of (25) is then recharacterized as in $S^R = \text{ascend}(S^R)$. Hence, both DC and f_s could be changed simultaneously, i.e.,

$$S^R(r) = \begin{cases} S^R(r - 1), & a = 1, i \neq r_{\min} \\ S^R(r + 1), & a = 3, i \neq r_{\max} \\ S^R(r), & \text{otherwise.} \end{cases} \quad (30)$$

In summary, intuitive solutions (28)–(30) regulate p^R and hence affect the evolution of (27).

D. Constrained Markov Decision Process

The constrained Markov decision process (CMDP) is applied into the sensor management system by setting a Markov-optimal policy u . This policy controls sensory sampling

operations by deciding which pair of DC and f_s need to be assigned in the sampling process, and it randomizes the decisions over given actions.

The CMDP parameter set is provided as follows.

- *Decision epochs* O are the outputs obtained from the context inference module. *State space* S^R and *action space* A are given by (25) and (24), respectively.
- *State transition probability* P_{rw}^a : This probability matrix defines transition probabilities among states $\{r \rightarrow w\}$ while action a is taken, i.e.,

$$P_{rw}^a = \begin{cases} \frac{1}{r-1}, & a = 1, w < r \\ 1, & a = 2, w = r \\ \frac{1}{W-r}, & a = 3, w > r \\ 0, & \text{otherwise.} \end{cases} \quad (31)$$

Remark that all transitions that form a specific state are set an equal probability according to the rule of actions. Different transition probabilities could bring an unfair selection of state.

- *Accuracy cost* $c(r, a)$: The accuracy cost is the retrieved error rate in user-state recognitions while the context inference framework is running, which is defined by ϕ in (22), and is given as follows:

$$c(r, a) = 1 - \phi_r^a. \quad (32)$$

On the other hand, the default settings for the accuracy cost is ruled by the rate of missing sampling points under different system states, where $\{(S = r)\} \rightarrow \{(\text{DC} = l) \times (f_s = k)\}$ and $\forall a \in A$

$$c(r, a)_{\text{default}} = c(\{l, k\}, a) = 1 - l + l \frac{k}{k_{\text{max}}}. \quad (33)$$

Remark that the default settings are the maximum error rates, indeed.

- *Power consumption* $d(r, a)$: The power consumption ratio is the reward process ψ_r .

$$d(r, a) = \psi_r \quad \forall a \in A. \quad (34)$$

The policy aims to maximize the accuracy in user-state recognitions subjected to the power constraints. Therefore, a CMDP distinguishes from a regular MDP in the added power consumption function d , which is related to the constraints V_y where $y \in [1, Y]$.

$\rho(r, a)$ is denoted in CMDP as the occupation measure by specifying the probability of a relevant state–action pair in the decision process, which satisfies the given constraints, whose probability distribution is given by

$$f(\gamma, u, r, a) = \sum_{t=1}^{\infty} \Pr_{\gamma}^u (S_t^R = r, A_t = a) \quad (35)$$

where γ and u are defined as any initial distribution and any stationary policy, respectively.

Having (31)–(34), the constrained optimization problem is given by the following requirements:

$$\min_{\rho} \sum_r \sum_a \rho(r, a) c(r, a)$$

$$\begin{aligned} \text{subject to } & \sum_r \sum_a \rho(r, a) (\delta_w(r) - P_{rw}^a) = 0, \\ & \sum_r \sum_a \rho(r, a) = 1, \rho(r, a) \geq 0 \end{aligned} \quad (36)$$

where $\forall r, w \in S^R, \forall a \in A, \delta_w(r) = \{1, r = w; 0, \text{otherwise}\}$.

Let u be the optimal policy that satisfies for all i, a , i.e.,

$$u_r(a) = \frac{\rho(r, a)}{\sum_a \rho(r, a)} \quad \forall r \in S, \forall a \in A \quad (37)$$

whenever the denominator is nonzero. Since the occupation measure is derived from

$$\begin{aligned} \rho(w) &= \gamma(w) + \sum_r \sum_{a(r)} \rho(w, a) P_{rw}^a \\ &= \gamma(w) + \sum_r \rho(r) \sum_{a(r)} \frac{\rho(w, a)}{\rho(r)} P_{rw}^a \\ &= \gamma(w) + \sum_r \rho(r) \sum_{a(r)} u_w(a) P_{rw}^a \\ &= \gamma(w) + \sum_r \rho(r) P_{rw}(u) \end{aligned} \quad (38)$$

it is concluded that ρ equals to $\gamma(I - P(u))^{-1}$ like defined in (36), and hence to (35), where I is the identity matrix.

In addition, the following constraints are added into (36):

$$\sum_i \sum_a \rho(r, a) d^y(r, a) \leq V_y, \quad y = 1, \dots, Y \quad (39)$$

where $V_y(t) = (1 \pm \nu)V_y(t - 1)$ is given for the constraint according to which action is taken, such as $\{a = 1 : -\nu\}$ and $\{a = 3 : +\nu\}$, where $0 < \nu < 1$ and $\{a = 2 : \nu = 0\}$.

Finally, the constrained optimization problem is defined from (36) and (39) as $\{\min c \text{ subject to } d^y \leq V_y\}$, whose solution is described in [30] and [31], and solved based on linear programming as follows: Find the minimum $C^* \in C(\gamma, u)$ for u defined in (37), $\rho \in f(\gamma, u)$ defined in (38), $C(\gamma, u) = C(\rho(u))$, and each $D^y(\gamma, u) = D^y(\rho(u))$, where the expected cost is expressed as in

$$\begin{aligned} C(\gamma, u) &= \mathbb{E}_{\gamma}^u \left\{ \sum_{t=1}^{\infty} c(S_t^R = r, A_t = a) \right\} \\ &= \sum_{t=1}^{\infty} \mathbb{E}_{\gamma}^u c(S_t^R = r, A_t = a) \\ &= \sum_{t=1}^{\infty} \sum_r \sum_{a_r} \Pr(S_t^R = r, A_t = a) c(r, a) \\ &= \sum_r \sum_{a_r} \sum_{t=1}^{\infty} \Pr(S_t^R = r, A_t = a) c(r, a) \\ &= \sum_r \sum_{a_r} f(\gamma, u, r, a) c(r, a). \end{aligned} \quad (40)$$

In the similar way, for the constraints

$$D^y(\gamma, u) = \sum_r \sum_{a_r} f(\gamma, u, r, a) d^y(r, a). \quad (41)$$

Under the policy u from (37) and derivation from (40) and (41), the expected average accuracy and power consumption cost is then defined by

$$\mathbb{E}^u[C] = \frac{1}{n} \sum_{n'=1}^n \mathbb{E}^u c_{n'}(i, a) \quad (42a)$$

$$\mathbb{E}^u[V] = \frac{1}{n} \sum_{\forall y} \sum_{n'=1}^n \mathbb{E}^u d_{n'}^y(i, a) \quad (42b)$$

where n' and n are the instant and total decision epoch times, respectively.

E. Partially Observable Markov Decision Process

The partially observable Markov decision process (POMDP) also describes an optimal solution to respond to the defined tradeoff. The parameter set by POMDP has some similarities such as the one provided by CMDP. The same states S^R , actions a , and state transitions P_{rw}^a are used in this model as well. A POMDP relies on an agent that takes some action $a \in A$ and hence makes the system moves from state r to a new state w . Due to the uncertainty in an action, the state transition is modeled by P_{rw}^a . In addition, the agent makes an observation $x \in O$ to gather information for the decision on the new system state selection; thereby, the state-observation relationship is probabilistically modeled by Z_{wx}^a . In each observation epoch, the agent takes action a in state r and then receives a reward $R(r, a)$.

The POMDP parameter set is given as follows.

- *Decision epochs* O , *state space* S^R , *action space* A , and *state transition probability* P_{rw}^a are given the same such as in Section V-D.
- *Observation emission probability* Z_{wx}^a : The observation is the accuracy ratio provided by the context inference module (see Section IV-B), i.e.,

$$Z_{wx}^a(t) = \frac{1}{|Z|} \begin{cases} \phi(t), & r = w \\ (1 - \phi(t)), & r \neq w \end{cases} \quad (43)$$

where $S_{(t-1)}^R = r$, $S_t^R = w$, $\forall a \in A$, $|Z| = \phi(t) + (W - 1)(1 - \phi(t))$, and $x = 1$ since there is only one observation, which is the accuracy ratio.

- *Reward function* $R_r^a(t)$: The reward process (i.e., power consumption) ψ_r is defined in Section V-A, i.e.,

$$R_r^a(t) = \psi_r \quad \forall a \in A. \quad (44)$$

- *Belief vector* $\lambda_r^a(t)$: Since the internal state of the underlying POMDP is not directly observable, the knowledge of the internal state could be provided by a belief vector $\lambda_r^a(t) \in \Lambda$ in the presence of the history of all past decisions and observations. The belief vector gives the conditional probability of being in state r under action a prior to any state transition.

The belief vector is updated whenever a new knowledge comes in after incorporating the action and observation obtained at time t within the history set of $\mathcal{H}(t) = \{a(\tau), O(\tau)\}$,

$\tau \in [1, t]$. The updated belief vector is obtained using (43) by the Bayes rule, i.e.,

$$\lambda_w^a(t+1) = \mathcal{T}(\lambda(t) | a, O) = \frac{Z_{wx}^a \sum_i P_{rw}^a \lambda_r^a(t)}{\sum_x Z_{wx}^a \sum_r P_{rx}^a \lambda_r^a(t)}. \quad (45)$$

The goal defined by POMDP is to develop an opportunistic sensor sampling strategy that seeks for a favorable tradeoff balance between accuracy in sensing and energy efficiency. Hence, a sensing policy $u^* : \Lambda \rightarrow A$ is defined to map a belief vector λ_r to an action a . The policy u^* is presented by a sequence of functions $\{u^* = [\eta_1, \eta_2, \dots, \infty]\}$, where η_t maps a belief vector $\lambda_r(t) \in \Lambda$ to an action $a \in A$ at time t over the infinite horizon of POMDP.

From the time at the current belief vector is $\lambda(t)$, a value function $V_t(\lambda(t))$ is denoted to represent the minimum expected remaining reward that can be earned under the assigned policies. This reward is obtained through immediate and future rewards. The optimal policy strikes a balance between earning immediate reward and obtaining a lean toward future decisions on the system.

The optimal strategy aims at minimizing the expected total reward, and it is defined together with (44) and (45) as

$$u = \arg \min_u \mathbb{E}_u \left[\sum_{t=1}^T R_r^a(t) | \lambda(1) \right]. \quad (46)$$

Hence, the value function for the total reward aggregation is given with the help of (46) as

$$V_t(\lambda(t)) = \min_a \mathbb{E} [R^a(\lambda(t)) + \varphi V_{t+1}(\mathcal{T}(\lambda(t) | a, S_r^a(t)))] \quad (47)$$

where $R^a(\lambda) = \sum_r \lambda_r R_r^a$, and $\varphi \in [0, 1]$ is a discount factor.

Due to the impact of the current action on the future rewards, an uncountable number of belief states lie over an infinite horizontal space. Therefore, specifying nonstationarity of the optimal policy or finding an optimal strategy for POMDP is often computationally prohibitive.

1) *Myopic Strategy and Sufficient Statistics*: Since finding an optimal strategy is computationally restricted, it is crucial to exploit the available POMDP and develop suboptimal strategies to reduce the complexity. Therefore, it is needed to show the *a posteriori* of distribution of the belief vector under sufficient statistics. The belief vector (45) is then updated based on the chosen action under the following sufficient statistics:

$$\lambda_r(t+1) = \begin{cases} (\lambda(t)_r^T P_{rw}^a)^T, & a' = \{1, 3\}, r \neq w \\ \lambda_i(t), & a' = 2, r = w \\ 0, & \text{otherwise} \end{cases} \quad (48)$$

where superscript T denotes the matrix transpose.

In addition, a myopic policy is introduced to ignore the impact of current action on the future rewards by solely focusing on minimizing the immediate reward. This is due to the fact that power consumption caused by instant sensory operation settings does not rely on future diversity in the sensory operation

methods. Thereby, the myopic policy makes $\varphi = 0$ in (47); hence, it turns (46) into

$$S_*^R = \arg \min_r \mathbb{E} [R_r^a(\lambda_r^a(t))] \\ \text{subjects to } \max(Z_{w,O=x}^a(t)) > \varepsilon \quad (49)$$

where S_*^R is the chosen optimal state, and ε denotes the minimum probability of given accuracy allowed by the process.

VI. PERFORMANCE EVALUATION

A case study in the HAR-based application model is examined to investigate the defined tradeoff by the proposed sensor management system. The targeted smartphone is placed fixed on user's hip area. A similar user activity profile is examined for each tradeoff analysis by five different participants. They are three males and two females, whose ages range from 18 to 30. Accordingly, the HAR-based user activity profile begins with a random activity pattern of user states *sitting* and *standing* for a minute (used for calibration); then, any of user states *sitting*, *standing*, *walking*, and *running* transits into the another one in the end of the following sojourn times of $\{5, 5, 10, 10, 30, 30, 60, 60, 100, 100, 300, 300\}$ s. This procedure is also performed three times (approximately 50 min in total per method by each individual) to see the effect of having a transition from longer waiting time to shorter waiting time, or *vice versa*. The initial 1-min-long application time is used for the adaptation process, which is reserved to set required adjustments in the system parameters with respect to the ongoing activity pattern. Note that system parameters already have default settings defined by (14). From this point, sensory operation parameters, which are DC and sampling frequency, are updated with a 10-s period. In addition, t_{suff} is set to 20 s. Recall that, as long as a continuing settlement time in any state is longer than t_{suff} , the sensor management system will decrease power consumption, which jeopardizes recognition accuracy of the activity pattern in return. The default sensory operation parameters are set to the aggressive sampling method, which is equal to the pair of $\{100\%, 100 \text{ Hz}\}$ for $\{\text{DC}, f_s\}$.

The context inference module is set to recognize a user state with a period of 1 s under the aggressive sampling method. The underlying Markovian chain in this module has a finite horizon length of 60, which means a-minute-long recent history of user states. Every 1 min, system parameters are updated according to (15). Except for the aggressive sampling method in sensory operations, the context inference module may not have a sensory observation at any time. For instance, in a case where the pair of $\{50\%, 50 \text{ Hz}\}$ is selected for sensory operation parameters, the decision period to recognize a user state is extended to 4 s, which results in having three empty decision points to estimate missing user-state recognitions.

The tradeoff analysis is carried out for each sensor management method by each participant. The tradeoff solutions by each method are averaged, and then shown in Fig. 4 for the analysis of power consumption ratio according to (27), (42b), and (47), and also in Fig. 5 for the analysis of averaged recognition accuracy according to (22), (42a), and (49). In addition, the tradeoff solutions by each method in both figures are noted by

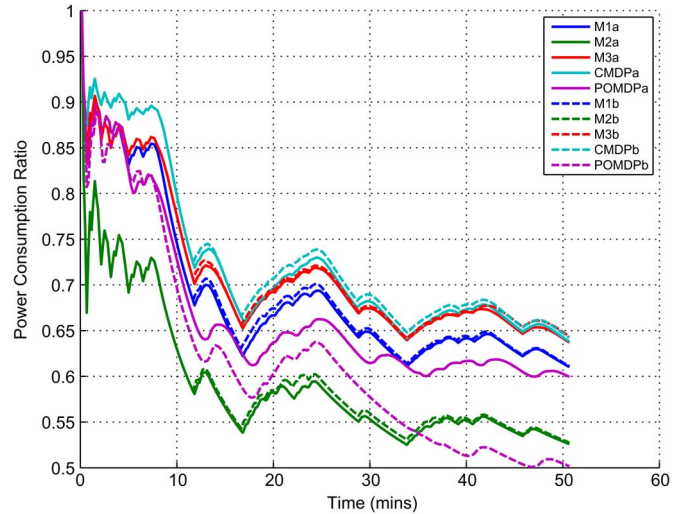


Fig. 4. Averaged power consumption ratio in response to user profile: The evolution of power consumption efficiency in comparison to the most aggressive sensory sampling methods is shown for each proposed sensory operation method in response to the analyzed user profile. Overall, 40% enhancement in power consumption caused by the smartphone accelerometer is achieved.

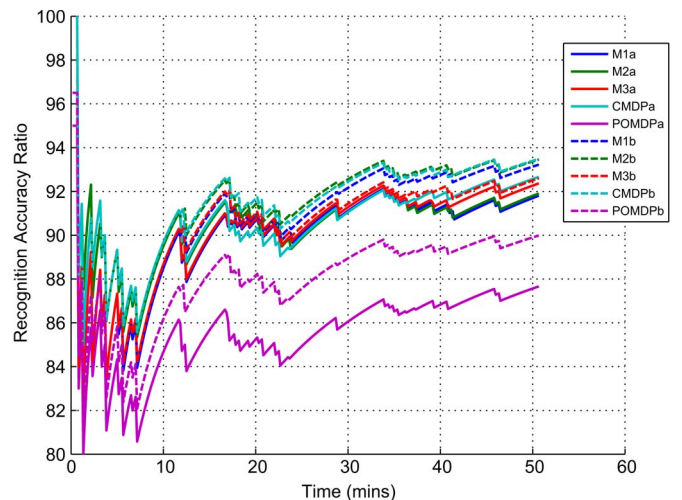


Fig. 5. Averaged recognition accuracy ratio in response to user profile. Having shown a drastic decrease initially due to the default system parameters, the recognition accuracy ratio heals gradually, while the context inference module gets better adaptation toward the analyzed user profiles and ends up with an overall 10%–15% decrease in accuracy ratio for user-state recognitions due to the proposed framework.

the suffixes “a” and “b” to demonstrate without/with some constraints added. The suffix “a” indicates the actual sensor management methods without any additional constraints. However, the suffix “b” sets extra rules on these methods. First, a 10% tolerance value is added into Methods I, II, and III to constrain the recognition accuracy ratio, which help the prevention of drastic recognition errors. If this constraint is exceeded, sensory operation parameters are forced to set the default settings, i.e., the aggressive sampling. Second, for CMDP, there is another constraint set on the power consumption ratio to control the tendency of the decision process to take an immoderate decrease in power consumption. According to this regulation, current sensory operation setting must stay in $\pm 25\%$ of the present power consumption level at most for the next setting. Finally, due to the additional constraint for POMDP, the update process

of the belief vector is reconfigured by adding the feature of $\lambda_i(t+1) = 1$, where $a = 2$.

In light of the explanations above, the following discussions can be made through both Figs. 4 and 5.

- Recognition accuracy ratio decreases significantly during the initial progress of context inference module since the framework begins running with default settings. Therefore, the adaptation process toward a user activity profile by the framework is not adequate yet. It is also because that users exhibit variant activity profiles that make the adaptation process take different time accordingly.
- Both figures show ups and downs, i.e., zigzag lines, to prove the defined tradeoff. This is because sensor management system always seeks for an opportunity to save in power consumption. However, this also jeopardizes the accuracy problem. In contrast, accuracy is healed by boosting power cost. Therefore, increase in power consumption compensates the worsening the recognition accuracy ratio, whereas decrease in power consumption receives benefits from the adaptation feature if possible where the framework shows high accuracy.
- When the time passes by and the framework gets a better adaptation to the user activity profile, the recognition accuracy ratio increases, although power consumption ratio decreases. It is also because at all user activities are known by the framework at this point and will lead to have continuity of better enhancement on tradeoff solutions.
- While switching from a longer waiting time to a slower waiting time, during the second or third run of the defined user activity pattern, accuracy decreases even if power consumption increases. It is because the system has been fully aware that the same user activity has been continuing for a longer waiting period. Moreover, it is also giving higher recognition accuracy compared with what it is currently available in the presence of higher-pace variant user activities.
- The recognition accuracy ratio may show a slight decrease if a state transition occurs after a long state visiting time or if the number of estimations in user-state recognition increases after a slower sampling policy is attained. This is because the entropy rate cannot converge into any stable point. In such cases, the framework attempts to fix the accuracy ratio.
- Among the intuitive solutions, a comparison can be made by $MIII > MI > MII$ in terms of the power consumption ratio and by $MI > MIII > MII$ in terms of the recognition accuracy ratio. Results show that the sampling in slower frequencies consume higher power than the sampling in lower DCs; however, it shows the opposite assumption for the recognition accuracy. It is because sampling in slower frequencies still obtains information about user activity while the sampling in lower DCs cannot do. On the other hand, MIII has the highest power consumption since it switches sensor operation modes modestly while achieving fine accuracy in user-state recognitions.
- $MXb > MXa$, where $X = I, II, III$ and $CMDPb > CMDPa$ are met in terms of the power consumption ratio due to the

fact that the aggressive sampling is forced to apply in case where severe errors occur in user-state recognitions.

- POMDPb makes a clear conclusion about the belief vector rather than POMDPa does when a sufficient visiting time elapsed on a specific user state. Hence, the power consumption decreases since the conclusion notifies the continuity of the same user state.
- MIII responds in a similar way that CMDP has while trying to reach their optimal policies.

In general, our novel tradeoff solutions achieve overall 40% enhancement in power consumption caused by the physical sensor work with respect to overall 10%–15% decrease in accuracy ratio for user-state recognitions due to the proposed generic context inference framework. The novelty of our framework also comes from the integrated adaptability feature toward variant user behaviors along with the online recognition accuracy tracker while providing optimal adaptive sampling strategies to achieve energy efficiency within the research area of mobile-device-based activity recognition. In contrast, some other recent studies within the same concept show enhancement in power efficiency by 20%–25% in [32], by 5%–10% in [33], and by 10%–30% in [34] while satisfying considerable recognition accuracy under nonadaptive, deterministic, and variant sampling frequency or DC applying sensor sampling methods.

VII. CONCLUSION

In this paper, a novel comprehensive framework has been presented within the futuristic concept of context awareness in mobile sensing. A statistical-machine-based context inference model together with an intelligent sensor management system is created to recognize human-centric activities. This approach aims at achieving a fine balance between power consumption and recognition accuracy. The study takes the smartphone accelerometer sensor into the scope to show the effectiveness of proposed total system structure, as well as leaving the door open for future improvements in the functionality of other smartphone sensors.

While creating the statistical machine, some features are taken into the consideration, such as time-varying user activity profile, system adaptability to the changing profile, nonuniform time distribution of sensory sampling process due to the power saving precautions, and the estimation process where missing sensory observations exist. On the other hand, while creating the sensor management system, the analytical modeling of power consumption caused by the accelerometer is examined. Thereby, along with the collaboration of the statistical machine, a better balance is achieved for the defined tradeoff throughout this paper. For the tradeoff analysis, some intuitive and optimal sensory operation solutions are provided to increase efficiency in power consumption, whereas the statistical machine tries to maintain the accuracy ratio provided by the framework.

REFERENCES

- [1] N. Lane *et al.*, "A survey of mobile phone sensing," *IEEE Commun. Mag.*, vol. 48, no. 9, pp. 140–150, Sep. 2010.
- [2] M. Baldauf, S. Dustdar, and F. Rosenberg, "A survey on context-aware systems," *Int. J. Ad Hoc Ubiquitous Comput.*, vol. 2, no. 4, pp. 263–277, Jun. 2007.

- [3] O. Yürür, C. H. Liu, and W. Moreno, "A survey of context-aware middleware designs for human activity recognition," *IEEE Commun. Mag.*, vol. 52, no. 6, pp. 24–31, Jun. 2014.
- [4] F.-J. Wu, Y.-F. Kao, and Y.-C. Tseng, "From wireless sensor networks towards cyber physical systems," *Pervasive Mobile Comput.*, vol. 7, no. 4, pp. 397–413, Aug. 2011.
- [5] C. Mascolo, L. Capra, and W. Emmerich, "Mobile computing middleware," in *Proc. Adv. Lect. Netw.*, 2002, pp. 506–510.
- [6] Y. Wang *et al.*, "A framework of energy efficient mobile sensing for automatic user state recognition," in *Proc. ACM MobiSys*, 2009, pp. 179–192.
- [7] H. Lu *et al.*, "The jigsaw continuous sensing engine for mobile phone applications," in *Proc. ACM SenSys*, 2010, pp. 71–84.
- [8] D. Siewiorek *et al.*, "Sensay: A context-aware mobile phone," in *Proc. IEEE ISWC*, 2003, p. 248.
- [9] S. Kang *et al.*, "SeeMon: Scalable and energy-efficient context monitoring framework for sensor-rich mobile environments," in *Proc. ACM MobiSys*, 2008, pp. 267–280.
- [10] A. Krause and C. Guestrin, "Optimal nonmyopic value of information in graphical models—Efficient algorithms and theoretical limits," in *Proc. Int. Joint Conf. Artif. Intell.*, 2005, pp. 1339–1345.
- [11] F. B. Abdesslem, A. Phillips, and T. Henderson, "Less is more: Energy-efficient mobile sensing with senseless," in *Proc. ACM MobiHeld*, 2009, pp. 61–62.
- [12] I. Constandache, S. Gaonkar, M. Sayler, R. Choudhury, and L. Cox, "EnLoc: Energy-efficient localization for mobile phones," in *Proc. IEEE INFOCOM*, Apr. 2009, pp. 2716–2720.
- [13] L. Atzori, A. Iera, and G. Morabito, "The Internet of things: A survey," *Comput. Netw.*, vol. 54, no. 15, pp. 2787–2805, Oct. 2010.
- [14] E. Kim, S. Helal, and D. Cook, "Human activity recognition and pattern discovery," *IEEE Pervasive Comput.*, vol. 9, no. 1, pp. 48–53, Jan.–Mar. 2010.
- [15] S. Zhong and J. Ghosh, "HMMS and coupled HMMS for multi-channel EEG classification," in *Proc. Int. Joint Conf. Neural Netw.*, 2002, vol. 2, pp. 1154–1159.
- [16] Z.-Y. He and L.-W. Jin, "Activity recognition from acceleration data using AR model representation and SVM," in *Proc. Int. Conf. Mach. Learn. Cybern.*, Jul. 2008, vol. 4, pp. 2245–2250.
- [17] L. Rabiner, "A tutorial on hidden Markov models and selected applications in speech recognition," *Proc. IEEE*, vol. 77, no. 2, pp. 257–286, Feb. 1989.
- [18] R. Pawula, "Generalizations and extensions of the Fokker-Planck-Kolmogorov equations," *IEEE Trans. Inf. Theory*, vol. IT-13, no. 1, pp. 33–41, Jan. 1967.
- [19] V. S. Barbu and N. Limnios, "Reliability of semi-Markov systems in discrete time: Modeling and estimation," in *Handbook of Performability Engineering*, K. B. Misra, Ed. London, U.K.: Springer-Verlag, 2008, pp. 369–380.
- [20] R. Pyke, "Markov renewal processes: Definitions and preliminary properties," *Ann. Math. Stat.*, vol. 32, no. 4, pp. 1231–1242, Dec. 1961.
- [21] G. D'amico, J. Janssen, and R. Manca, "Duration dependent semi-Markov models," *Appl. Math. Sci.*, vol. 5, no. 42, pp. 2097–2108, 2011.
- [22] S. E. Levinson, "Continuously variable duration hidden Markov models for automatic speech recognition," *Comput. Speech Lang.*, vol. 1, no. 1, pp. 29–45, Mar. 1986.
- [23] S.-Z. Yu and H. Kobayashi, "A hidden semi-Markov model with missing data and multiple observation sequences for mobility tracking," *Signal Process.*, vol. 83, no. 2, pp. 235–250, Feb. 2003.
- [24] O. Cappé, E. Moulines, and T. Ryden, *Inference in Hidden Markov Models (Springer Series in Statistics)*. New York, NY, USA: Springer-Verlag, 2005.
- [25] G. Ciuperca and V. Girardin, "Estimation of the entropy rate of a countable Markov chain," *Commun. Stat. Theory Methods*, vol. 36, no. 13–16, pp. 2543–2557, Oct. 2007.
- [26] ADXL346 3-Axis 2 G Ultra Low Power Digital Accelerometer by Analog Devices. [Online]. Available: <http://www.analog.com/en/mems-sensors/mems-inertial-sensors/adxl346/products/product.html>
- [27] O. Yurur, C. H. Liu, and W. Moreno, "Unsupervised posture detection by smartphone accelerometer," *Electron. Lett.*, vol. 49, no. 8, pp. 562–564, Apr. 2013.
- [28] V. Rao, G. Singhal, A. Kumar, and N. Navet, "Battery model for embedded systems," in *Proc. IEEE VLSID*, 2005, pp. 105–110.
- [29] O. Yurur and W. Moreno, "Energy efficient sensor management strategies in mobile sensing," in *Proc. ISTE Gener. Assem.*, May 2011, pp. 66–72.
- [30] E. Altman, *Constrained Markov Decision Processes*. New York, NY, USA: Taylor & Francis, 1999, Stochastic Modeling Series.
- [31] M. L. Puterman, *Markov Decision Processes: Discrete Stochastic Dynamic Programming.*, First ed. Hoboken, NJ, USA: Wiley, 1994.
- [32] Z. Yan, V. Subbaraju, D. Chakraborty, A. Misra, and K. Aberer, "Energy-efficient continuous activity recognition on mobile phones: An activity-adaptive approach," in *Proc. ISWC*, Jun. 2012, pp. 17–24.
- [33] F. Casamassima, E. Farella, and L. Benini, "Context aware power management for motion-sensing body area network nodes," in *Proc. DATE*, Mar. 2014, pp. 1–6.
- [34] V. Srinivasan and T. Phan, "An accurate two-tier classifier for efficient duty-cycling of smartphone activity recognition systems," in *Proc. ACM PhoneSense*, 2012, pp. 11:1–11:5.



Özgür Yürür (M'13) received the Double Major degree from Gebze Institute of Technology, Kocaeli, Turkey, in 2008 and the M.S.E.E. and Ph.D. degrees from the University of South Florida, Tampa, FL, USA, in 2010 and 2013, respectively.

He is currently with RF Micro Devices, Greensboro, NC, USA, where he is responsible for research and design of new test development strategies, as well as for the implementation of hardware, software, and firmware solutions for second-, third-, and fourth-generation and wireless-

based company products. His research interests include ubiquitous sensing, mobile computing, machine learning, and energy-efficient optimal sensing policies in wireless networks.



Chi Harold Liu (M'10) received the B.Eng. degree from Tsinghua University, Beijing, China, and the Ph.D. degree from Imperial College London, London, U.K.

He is currently a Full Professor with the School of Software, Beijing Institute of Technology. He is also the Director of the IBM Mainframe Excellence Center, Beijing; the Director of the IBM Big Data Technology Center; and the Director of the National Laboratory of Data Intelligence for China Light Industry. Before moving to academia, he joined IBM

Research-China as a Staff Researcher and a Project Manager, after working as a Postdoctoral Researcher with Deutsche Telekom Laboratories, Germany, and as a Visiting Scholar the IBM T. J. Watson Research Center, Yorktown Heights, NY, USA. He is the author of more than 60 prestigious conference and journal papers and is the holder of more than ten EU/U.S./China patents. His current research interests include the Internet of Things, big data analytics, and mobile computing.

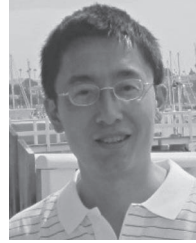
Dr. Liu served as the General Chair for the 2013 IEEE International Conference on Sensing, Communication, and Networking Workshop on internet-of-things (IoT) Networking and Control, the 2013 IEEE Wireless Communications and Networking Conference Workshop on IoT Enabling Technologies, and the 2011 Association for Computing Machinery (ACM) International Conference on Ubiquitous Computing Workshop on Networking and Object Memories for IoT. He served as the Consultant to the Asian Development Bank, Bain & Company, and KPMG, USA, as well as the Peer Reviewer for the Qatar National Research Foundation and the National Science Foundation, China. He serves as the Editor for the *KSII Transactions on Internet and Information Systems* and as the Book Editor for four books published by Taylor & Francis Group, USA. He received the Distinguished Young Scholar Award in 2013, the IBM First Plateau Invention Achievement Award in 2012, and the IBM First Patent Application Award in 2011. He was interviewed by EEWeb.com as the Featured Engineer in 2011. He is a member of ACM.



Charith Perera received the B.Sc. (Hons) degree in computer science from Staffordshire University, Stoke-on-Trent, U.K. in 2009 and the Master's degree in business administration from the University of Wales, Cardiff, U.K. in 2012. He is currently working toward the Ph.D. degree in computer science with The Australian National University, Canberra, Australia.

He is also with the Information Engineering Laboratory, ICT Centre, CSIRO, Australia, where he is involved in the EU Open source blueprint for large-scale self-organizing cloud environments for IoT applications (FP7 OpenIoT) Project. His research interests include Internet of Things, pervasive and ubiquitous computing with a focus on sensor networks, middleware, context-aware computing, mobile computing, and semantic technologies.

Dr. Perera is a member of the Association for Computing Machinery.



Xue Liu (M'06) received the B.S. degree in mathematics and the M.S. degree in automatic control from Tsinghua University, Beijing, China, and the Ph.D. degree in computer science from the University of Illinois at Urbana-Champaign, Champaign, IL, USA, in 2006.

He worked as the Samuel R. Thompson Associate Professor with the University of Nebraska-Lincoln, Lincoln, NE, USA, and has also worked with HP Labs, Palo Alto, CA, USA. He is currently an Associate Professor with the School of Computer Science, McGill University, Montreal, QC, Canada. He is the author of more than 150 research papers in major peer-reviewed international journals and conference proceedings. He is the holder of one U.S. patent and has filed four other U.S. patents. His research interests include computer networks and communications, smart grid, real-time and embedded systems, cyber-physical systems, data centers, and software reliability.

Dr. Liu received the 2008 Best Paper Award from the IEEE TRANSACTIONS ON INDUSTRIAL INFORMATICS and the First Place Best Paper Award at the 2011 Association for Computing Machinery Conference on Wireless Network Security.



Min Chen (SM'09) received the Ph.D. degree from South China University of Technology, China, in 2004.

He was an Assistant Professor with Seoul National University, Seoul, Korea. He is currently a Full Professor with the School of Computer Science and Engineering, Huazhong University of Science and Technology, Wuhan, China. He is the author of more than 150 papers. His research interests include multimedia and communications, such as multimedia transmission over wireless networks, wireless sensor

networks, body sensor networks, radio-frequency identification, ubiquitous computing, intelligent mobile agents, pervasive computing and networks, E-healthcare, medical application, machine-to-machine communications, Internet of Things, etc.

Mr. Chen served as a Cochair of the 2012 IEEE International Conference on Communications (ICC) Communications Theory Symposium and of the IEEE ICC 2013 Wireless Networks Symposium. He currently serves as a General Cochair for the 2012 12th IEEE International Conference on Computer and Information Technology. He serves as an Editor or an Associate Editor for *Wireless Communications and Mobile Computing*, *IET Communications*, *IET Networks*, the *Wiley International Journal of Security and Communication Networks*, the *Journal of Internet Technology*, the *KSII Transactions on Internet and Information Systems*, and the *International Journal of Sensor Networks*. He is a Managing Editor for the *International Journal of Autonomous and Adaptive Communications Systems*.



Wilfrido Moreno received the B.S.E.E., M.S.E.E., and Ph.D. degrees from the University of South Florida (USF), Tampa, FL, USA.

He is currently a Professor with the Department of Electrical Engineering, USF, and is the Director for the Ibero-American Science and Technology Educational Consortium at USF (ISTEC-USF). In addition, he has served as the Director of the R&D Initiative for ISTEC Inc. since the fall of 2003. In the area of research, he is a founding member of the former Center for Microelectronics Research, which is currently the Nanotechnology Research and Education Center. Currently, he has supervised industrial projects applying system of systems engineering methodologies. His broad educational background in communication, systems and controls, and micro/nanoelectronics has allowed him to work on multidisciplinary research projects where concepts and expertise in all of these areas comes together for system design, fabrication, and test. His research interests include system integration by providing "off-the-shelf" hardware/software solutions to industrial applications. His application interests include digital signal processing, communications, industrial power and controls, nano/microelectronics, biomedical engineering and multimedia solutions, and optimal sensing.

Dr. Moreno has participated in over 150 International conferences and seminars around the world and has organized more than 50 hands-on workshops in the area of electronic design automation, systems engineering and controls, nanoelectronics, and digital signal processing.